Lecture 17. Temperature Lidar (5) Boltzmann Technique and Rotational Raman Technique

- Introduction
- Boltzmann temperature technique
- Fe Boltzmann temperature lidar
- N_2^+ Boltzmann temperature lidar
- Rotational Raman lidar
- Summary

Introduction

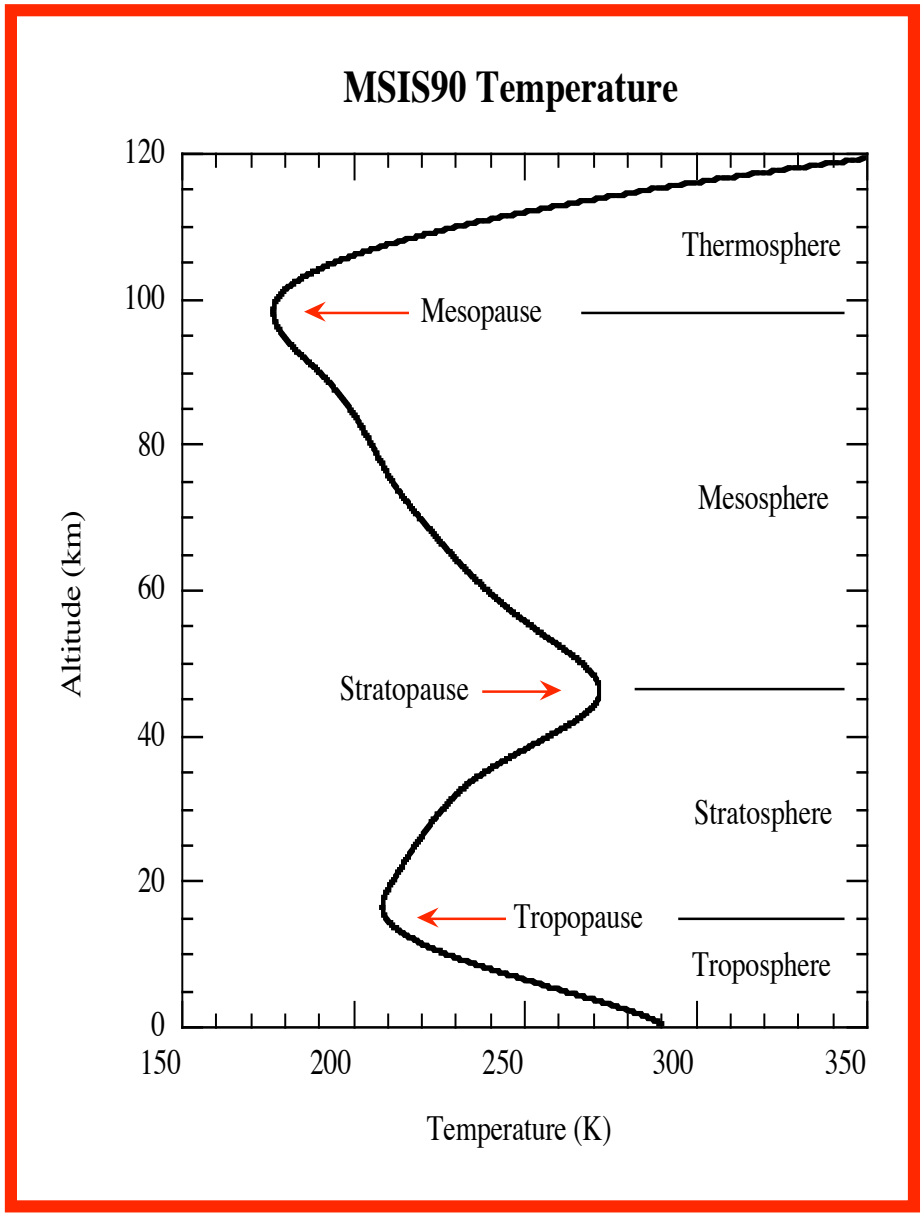

- Resonance fluorescence lidar technique can be used in MLT region, and also extended to thermosphere on molecular species, like N_2^+

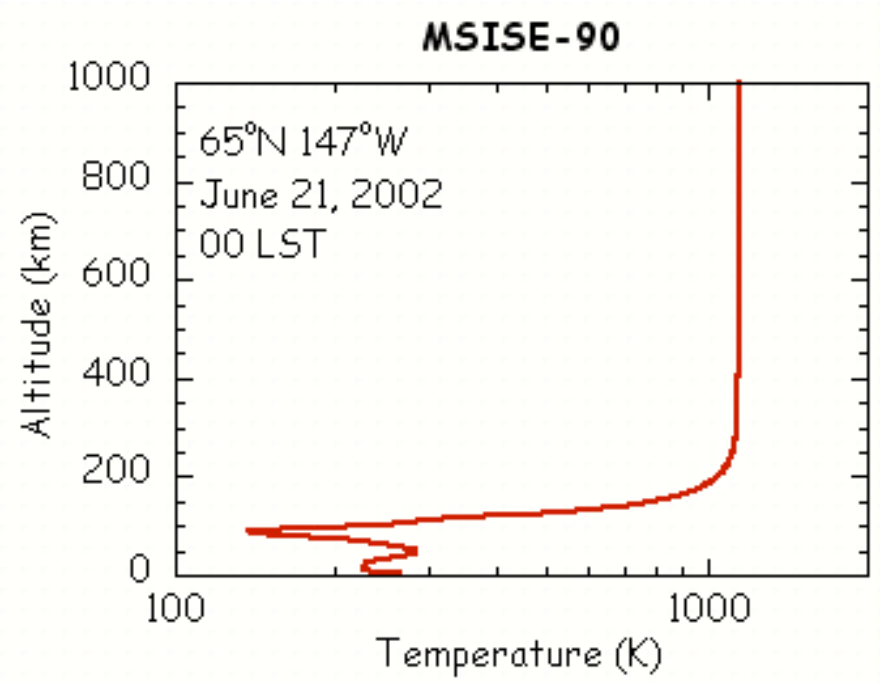

- How about lower atmos with aerosols? - Raman, HSRL, & DIAL

Boltzmann Temperature Technique

- Boltzmann distribution is the law of particle population distribution according to energy levels under thermodynamic equilibrium (Maxwell-Boltzmann distribution law)

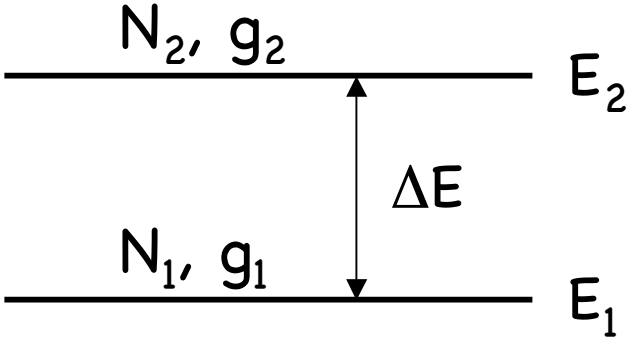

$$\frac{N_2}{N_1} = \frac{g_2}{g_1}\exp\left\{-\left(E_2 - E_1\right)/k_B T\right\}$$

$$\frac{N_k}{N} = \frac{g_k \exp(-E_k/k_B T)}{\sum_i g_i \exp(-E_i/k_B T)}$$

$$T = \frac{\Delta E/k_B}{\ln\left(\frac{g_2}{g_1}\cdot\frac{N_1}{N_2}\right)}$$

N_1 and N_2 - particle populations on energy levels E_1 and E_2
g_1 and g_2 - degeneracy for energy levels E_1 and E_2, $\Delta E = E_2 - E_1$
k_B - Boltzmann constant, T - Temperature, N - total population

Population Ratio ⇨ Temperature

Fe Atomic Energy Levels

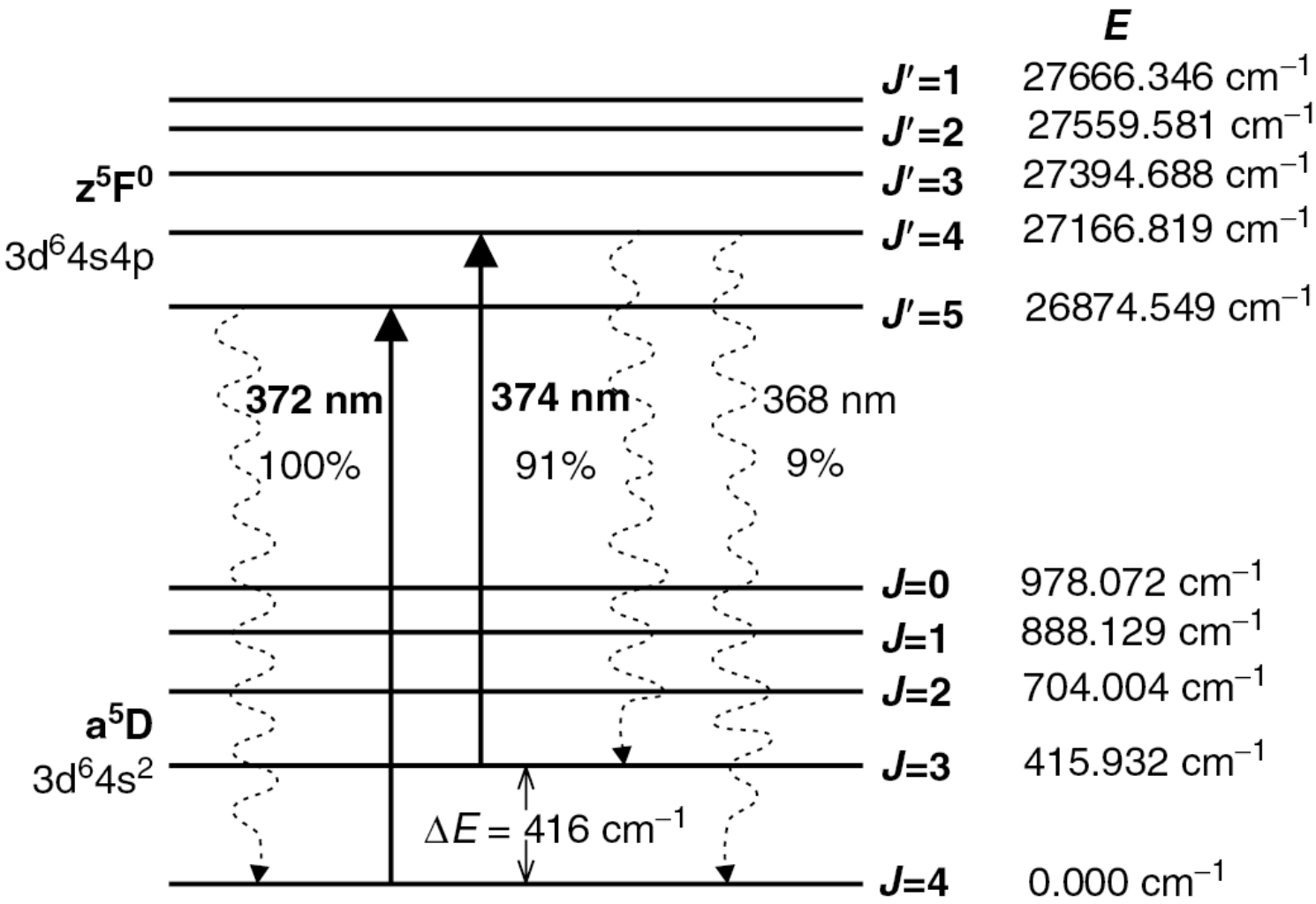

Fluorescence Intensity Ratio ⇨ Population Ratio ⇨ Temperature

Fe Atomic Parameters

Table 5.3 Isotopic Data of Fe Atoms

	^{54}Fe	^{56}Fe	^{57}Fe	^{58}Fe
Z	26	26	26	26
A	54	56	57	58
Nuclear spin	0	0	1/2	0
Natural abundance	5.845%	91.754%	2.119%	0.282%

Table 5.4 Fe Resonance Line Parameters

Transition wavelength λ	372.0993 nm	373.8194 nm
Degeneracy for ground state	$g_1 = 9$	$g_2 = 7$
Degeneracy for excited state	$g_1' = 11$	$g_2' = 9$
Radiative lifetime of excited state (ns)	61.0	63.6
Einstein coefficient A_{ki} (10^8 s^{-1})	0.163	0.142
Oscillator strength f_{ik}	0.0413	0.0382
Branching ratio R_B	0.9959	0.9079
σ_0 (10^{-17} m^2)	9.4	8.7

Fe Boltzmann Lidar Principle

$$N_{\mathrm{Fe}}(\lambda,z) = \left(\frac{P_{\mathrm{L}}\Delta t T_{\mathrm{a}}}{hc/\lambda}E(\lambda,z)\right)\sigma_{\mathrm{eff}}(\lambda,T,\sigma_{\mathrm{L}})R_{\mathrm{B}\lambda}\rho_{\mathrm{Fe}}(\lambda,z)$$
$$\times\Delta z\left(E(\lambda,z)T_{\mathrm{a}}\frac{A_{\mathrm{R}}}{4\pi z^2}\eta\right) \qquad (5.92)$$

$$N_{\mathrm{norm}}(\lambda,z) = \frac{N_{\mathrm{Fe}}(\lambda,z)+N_{\mathrm{B}}(\lambda,z)-\hat{N}_{\mathrm{B}}(\lambda)}{N_{\mathrm{R}}(\lambda,z_{\mathrm{R}})+N_{\mathrm{B}}(\lambda,z_{\mathrm{R}})-\hat{N}_{\mathrm{B}}(\lambda)}$$
$$= \frac{z_{\mathrm{R}}^2E^2(\lambda,z)R_{\mathrm{B}\lambda}\sigma_{\mathrm{eff}}(\lambda,T,\sigma_{\mathrm{L}})\rho_{\mathrm{Fe}}(\lambda,z)}{z^2\sigma_{\mathrm{R}}(\lambda)\rho_{\mathrm{atmos}}(z_{\mathrm{R}})}$$

Fe Boltzmann Lidar Principle

$$
\begin{aligned}
R_{\mathrm{T}}(z) &= \frac{N_{\mathrm{norm}}(\lambda_{374}, z)}{N_{\mathrm{norm}}(\lambda_{372}, z)} \\
&= \frac{g_2}{g_1} \frac{R_{\mathrm{B374}}}{R_{\mathrm{B372}}} \left(\frac{\lambda_{374}}{\lambda_{372}}\right)^{4.0117} \frac{E^2(\lambda_{374}, z)}{E^2(\lambda_{372}, z)} \\
&\quad \times \frac{\sigma_{\mathrm{eff}}(\lambda_{374}, T, \sigma_{\mathrm{L374}})}{\sigma_{\mathrm{eff}}(\lambda_{372}, T, \sigma_{\mathrm{L372}})} \exp(-\Delta E / k_{\mathrm{B}} T)
\end{aligned}
$$

$$
R_{\sigma} = \frac{\sigma_{\mathrm{eff}}(\lambda_{374}, T, \sigma_{\mathrm{L374}})}{\sigma_{\mathrm{eff}}(\lambda_{372}, T, \sigma_{\mathrm{L372}})}
$$

$$
R_E(z) = \frac{E(\lambda_{374}, z)}{E(\lambda_{372}, z)}
$$

$$
\begin{aligned}
T(z) &= \frac{\Delta E / k_{\mathrm{B}}}{\ln\left[\frac{g_2}{g_1} \frac{R_{\mathrm{B374}}}{R_{\mathrm{B372}}} \left(\frac{\lambda_{374}}{\lambda_{372}}\right)^{4.0117} \frac{R_E^2(z) R_{\sigma}}{R_{\mathrm{T}}(z)}\right]} \\
&= \frac{598.44K}{\ln\left[\frac{0.7221 R_E^2(z) R_{\sigma}}{R_{\mathrm{T}}(z)}\right]}
\end{aligned}
$$

Fe Boltzmann Lidar Calibration and Sensitivity Analysis

$$R_{\mathrm{T}}(z) = \frac{N_{\mathrm{norm}}(\lambda_{374}, z)}{N_{\mathrm{norm}}(\lambda_{372}, z)} = \frac{g_2}{g_1}\frac{R_{\mathrm{B374}}}{R_{\mathrm{B372}}}\left(\frac{\lambda_{374}}{\lambda_{372}}\right)^{4.0117}\frac{E^2(\lambda_{374}, z)}{E^2(\lambda_{372}, z)} \times \frac{\sigma_{\mathrm{eff}}(\lambda_{374}, T, \sigma_{\mathrm{L374}})}{\sigma_{\mathrm{eff}}(\lambda_{372}, T, \sigma_{\mathrm{L372}})}\exp(-\Delta E/k_{\mathrm{B}}T)$$

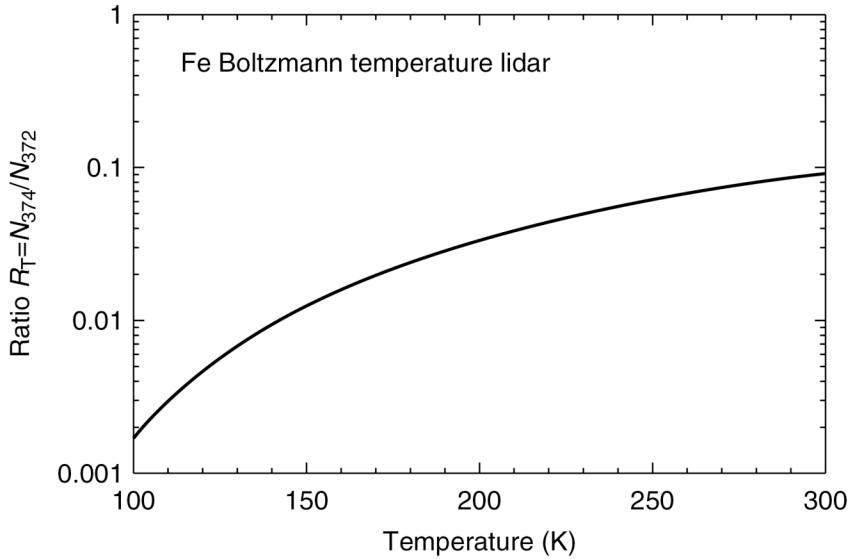

$$S_{\mathrm{T}} = \frac{\partial R_{\mathrm{T}}/\partial T}{R_{\mathrm{T}}}$$

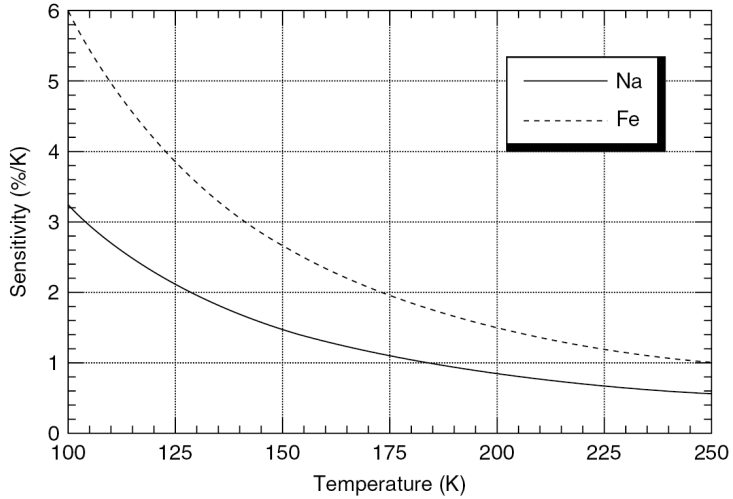

Fe Boltzmann Lidar Instrumentation

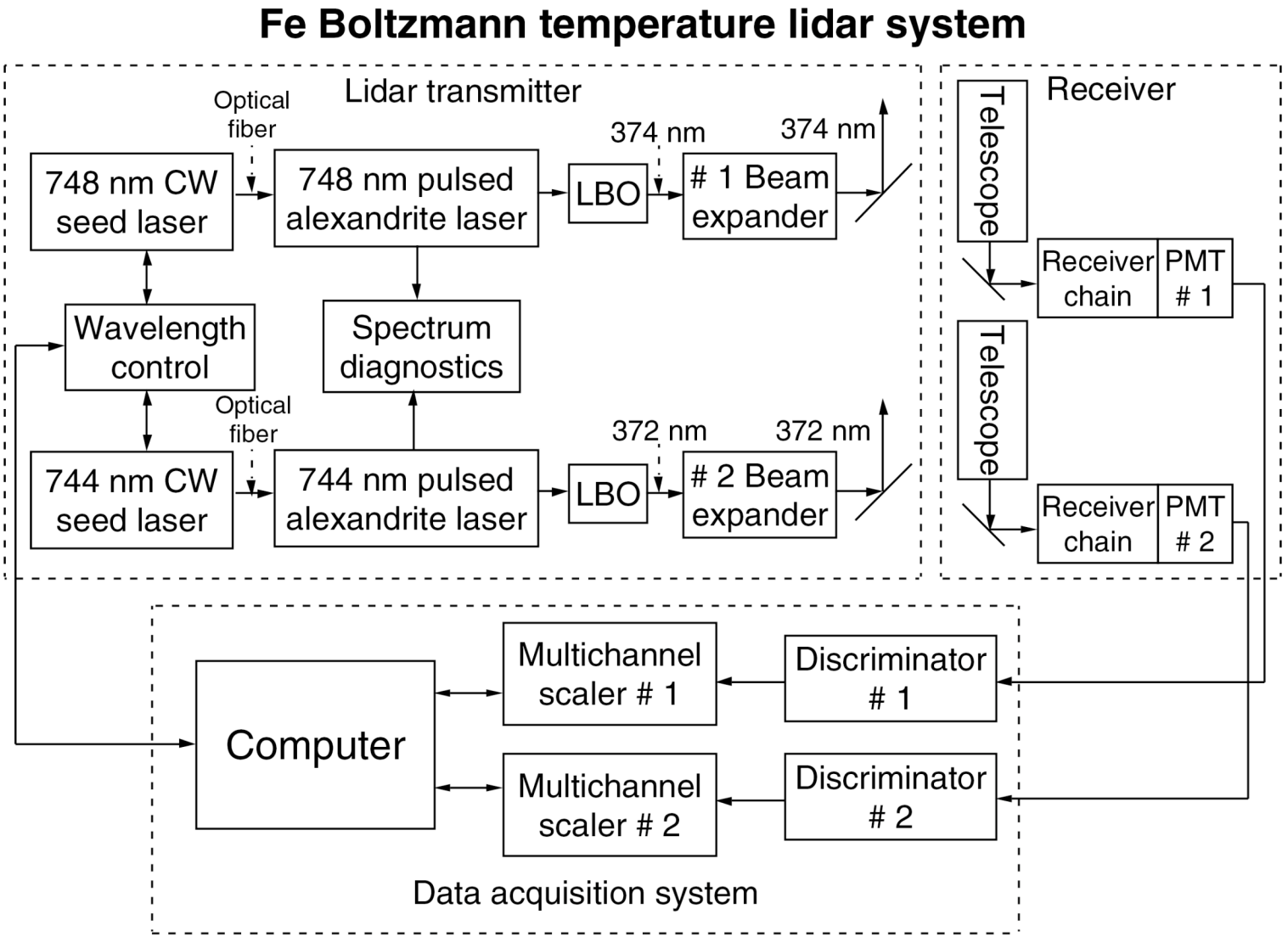

Fe Boltzmann Lidar Transmitter

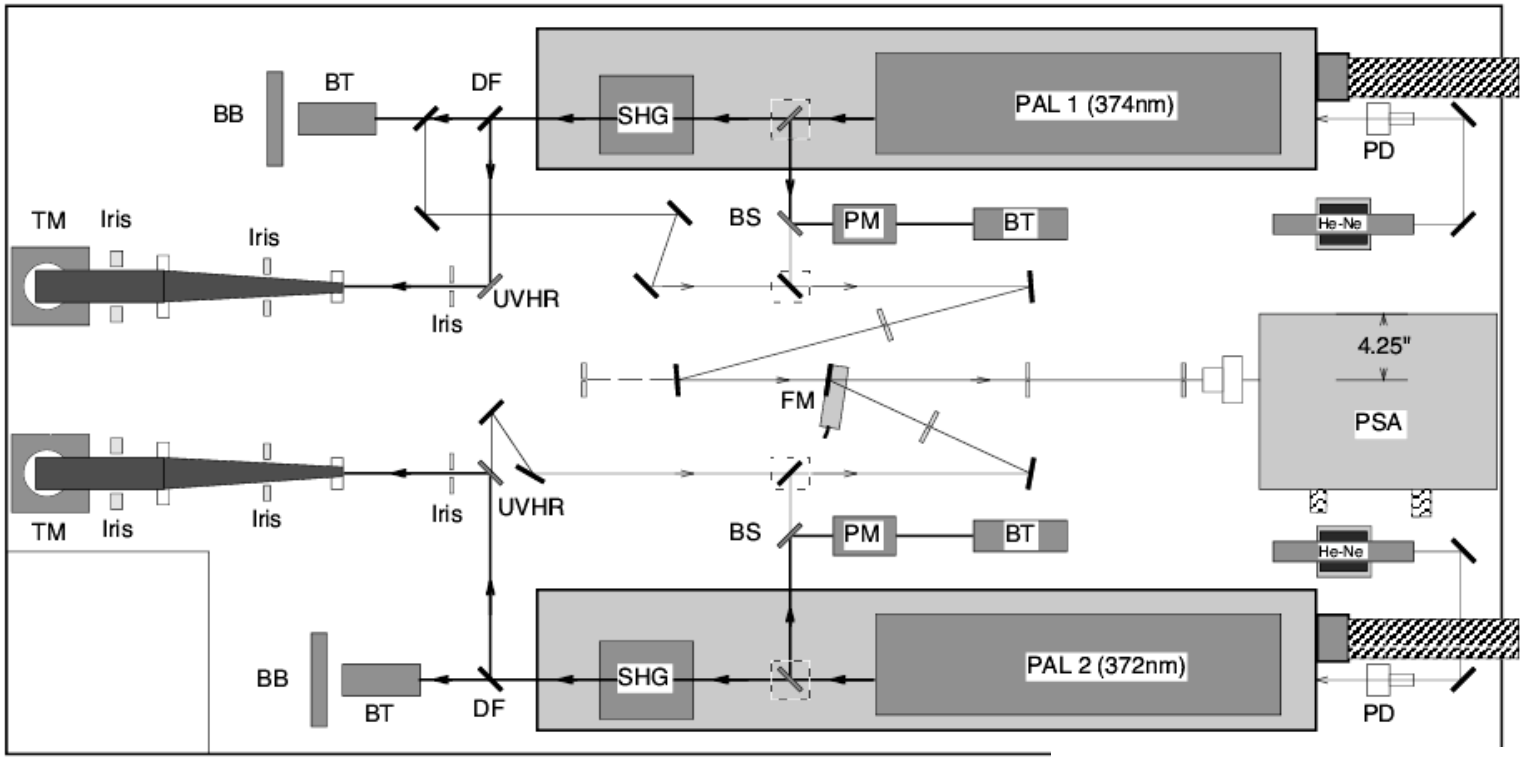

- Based on injection-seeded, frequency-doubled, pulse Alexandrite laser systems (output at 372 and 374 nm)

Seeder Laser Structure and Wavelength Control

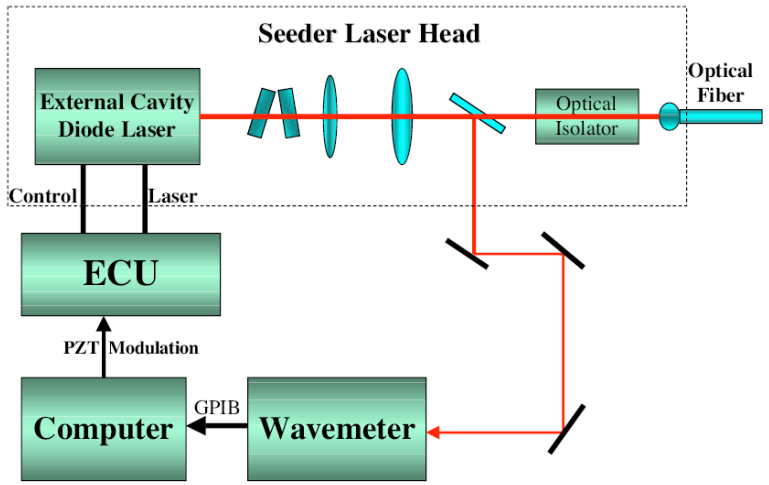

Fe Boltzmann Lidar @ South Pole

Fe Boltzmann Lidar @ Rothera

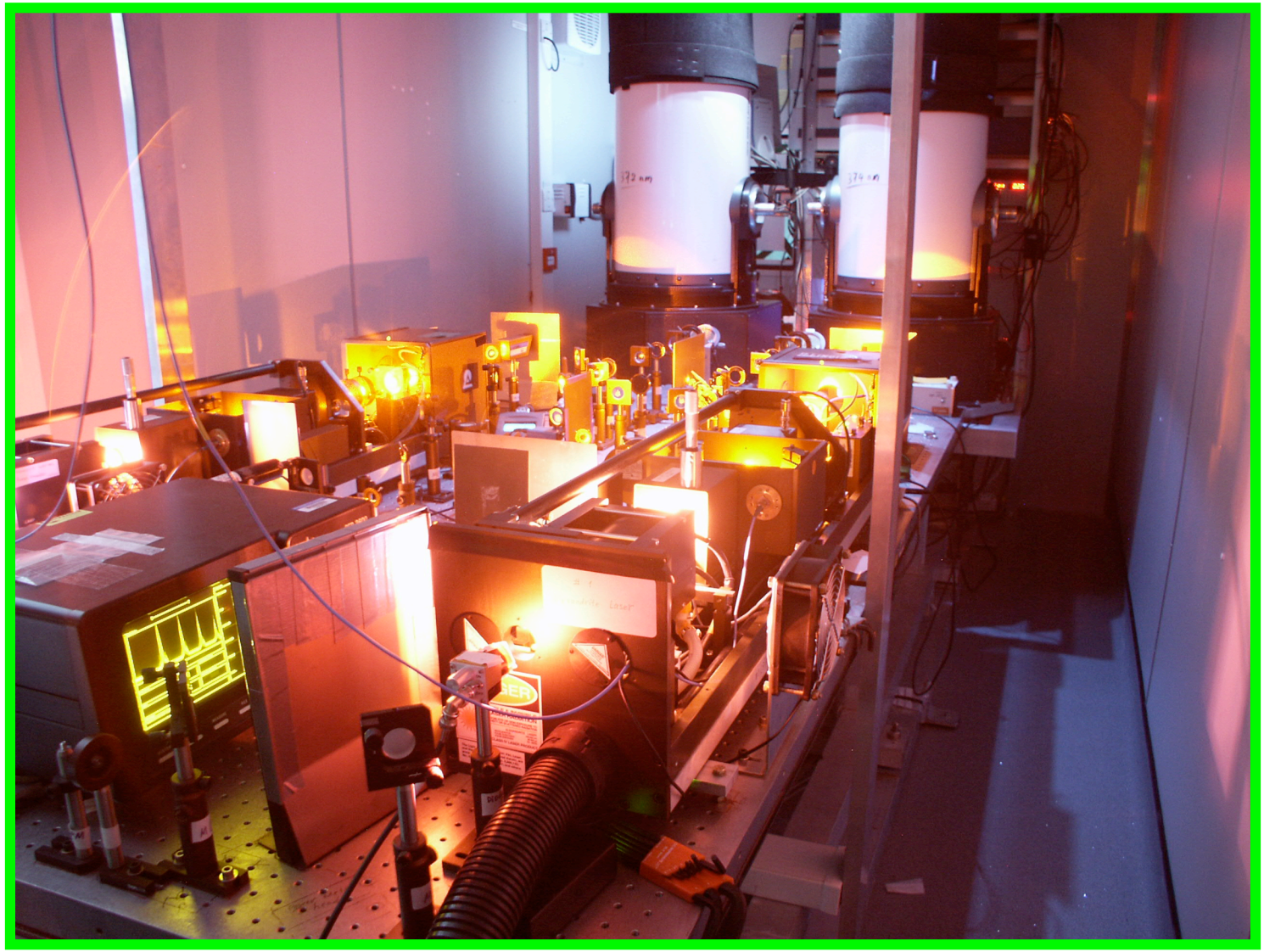

Fe Boltzmann Lidar Receiver

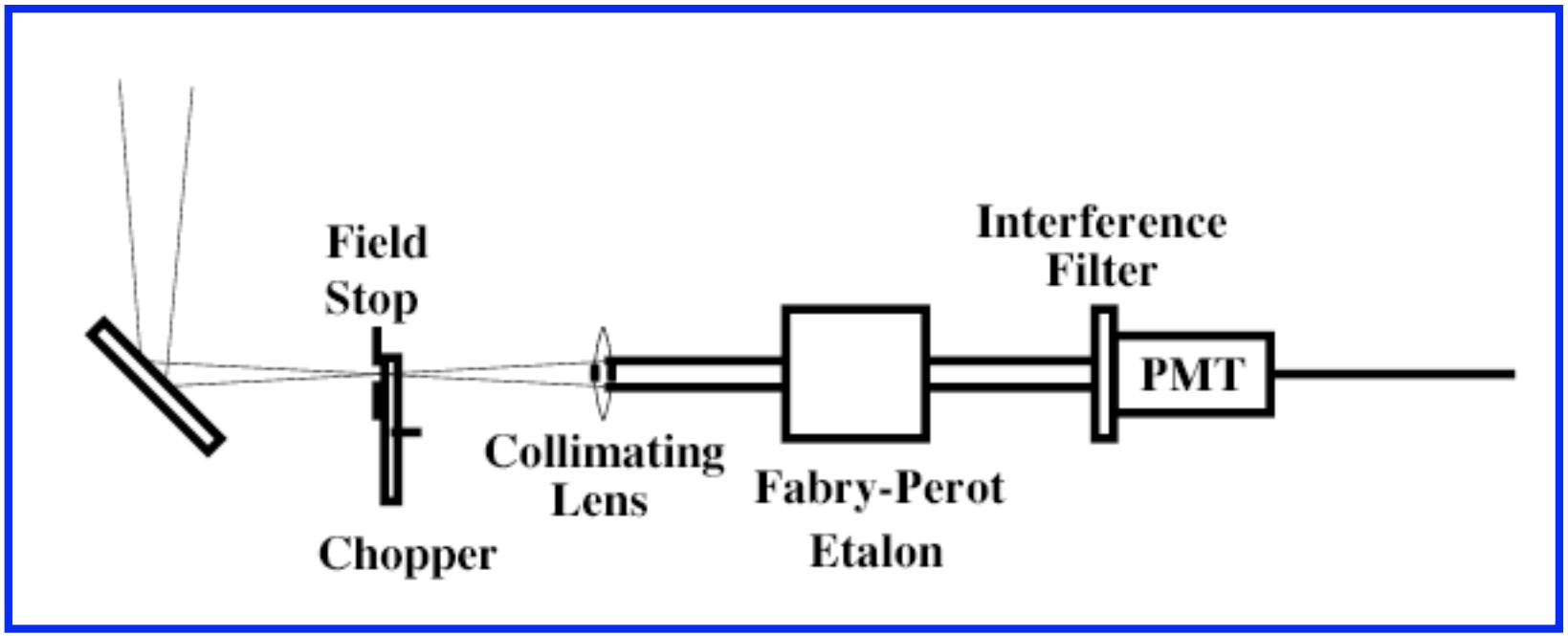

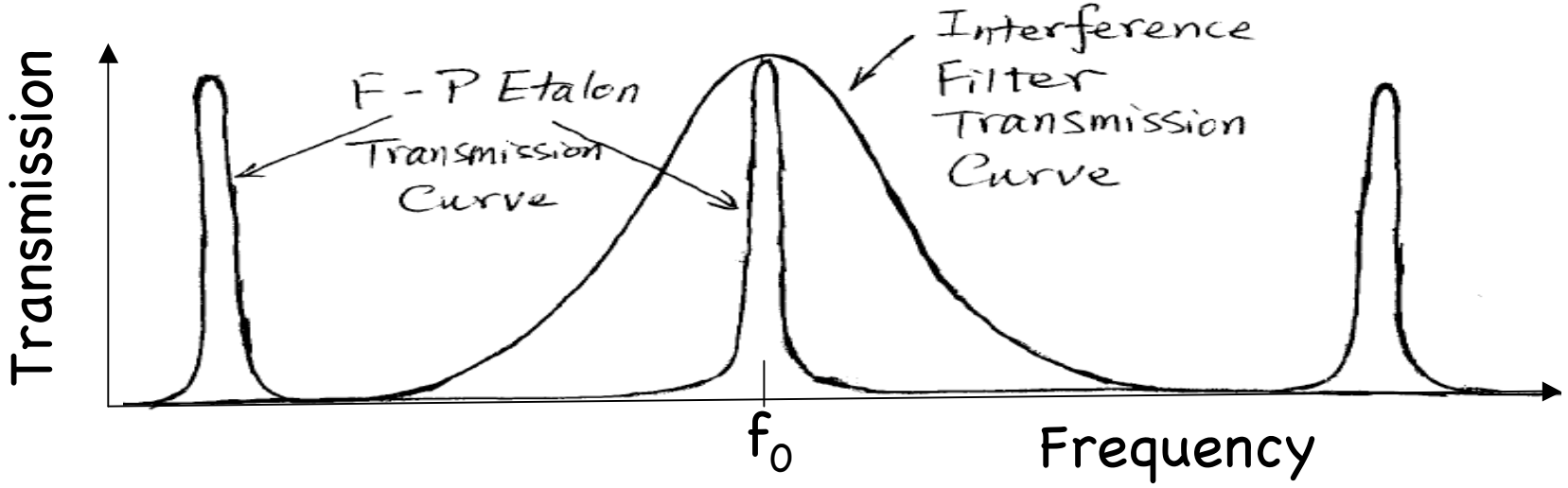

Fe Boltzmann Lidar Receiver

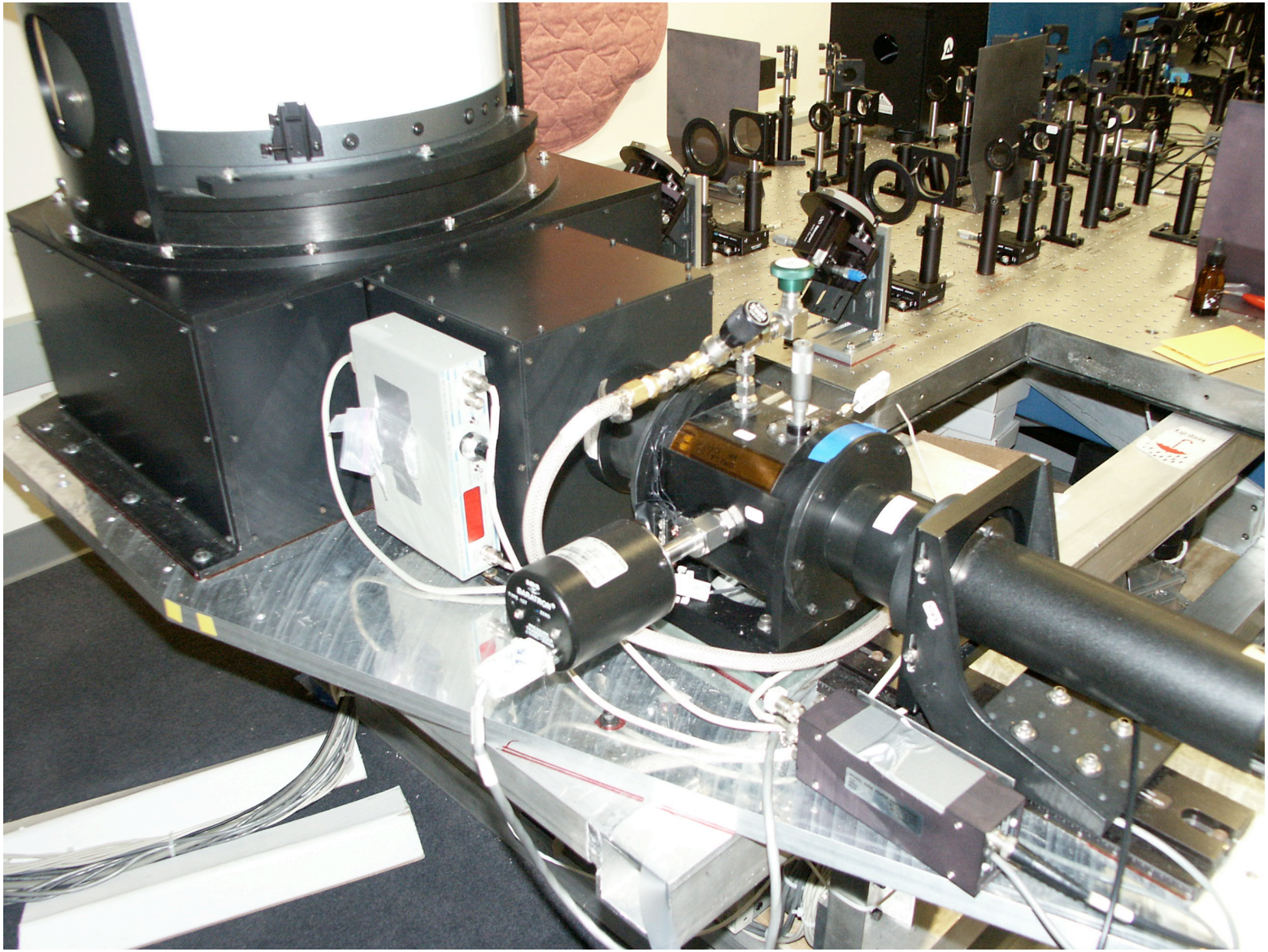

The Ionosphere and Thermosphere

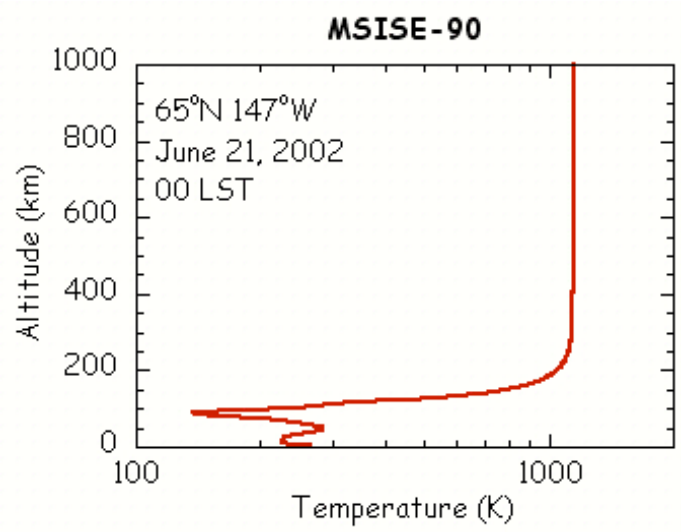

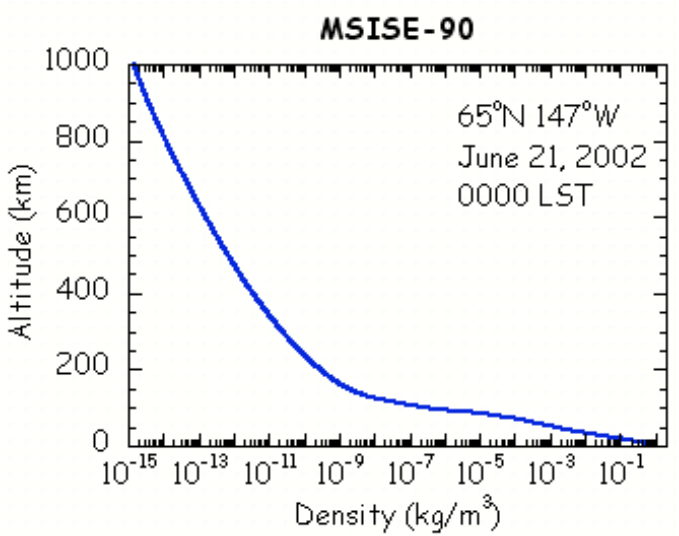

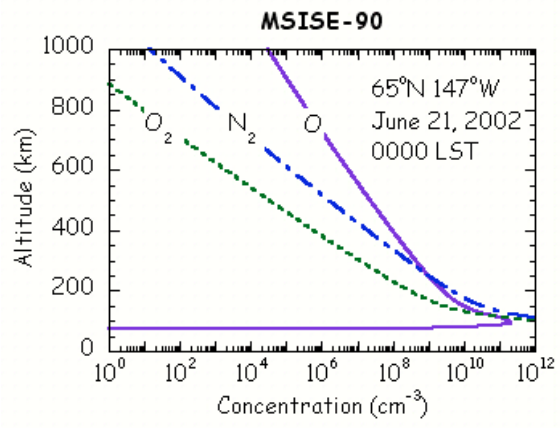

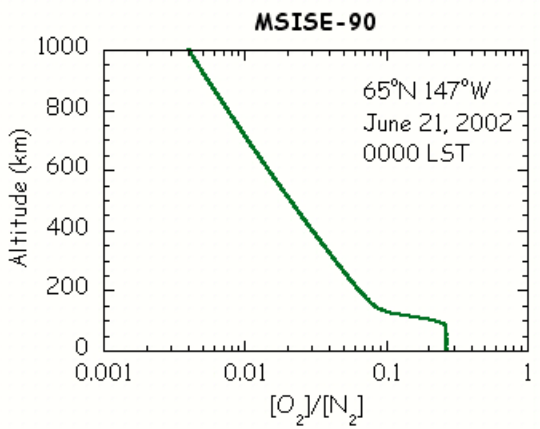

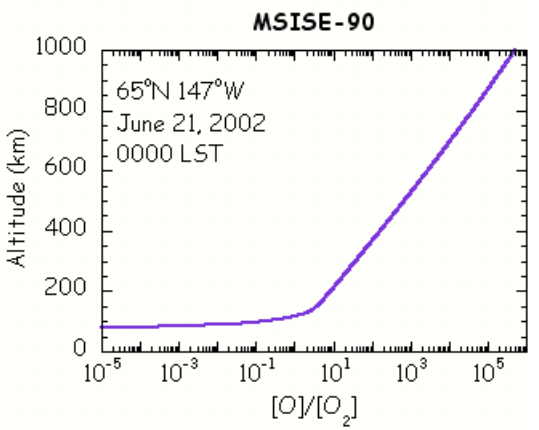

Courtesy to Richard Collins of UAF

The Aurorally-Modified Ionosphere

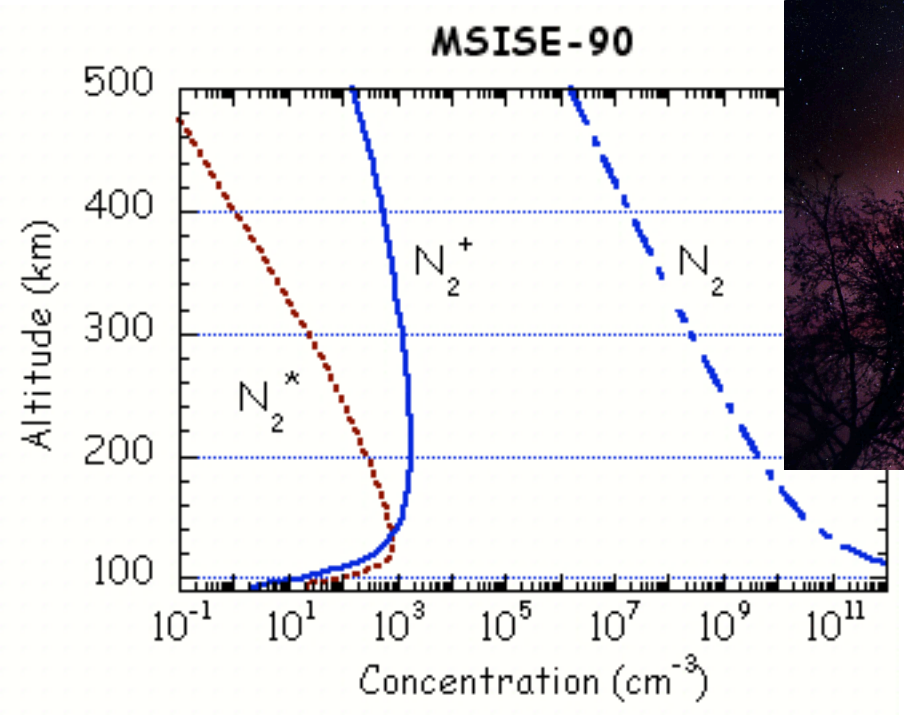

Photo courtesy of GI-UAF by Jan Curtis

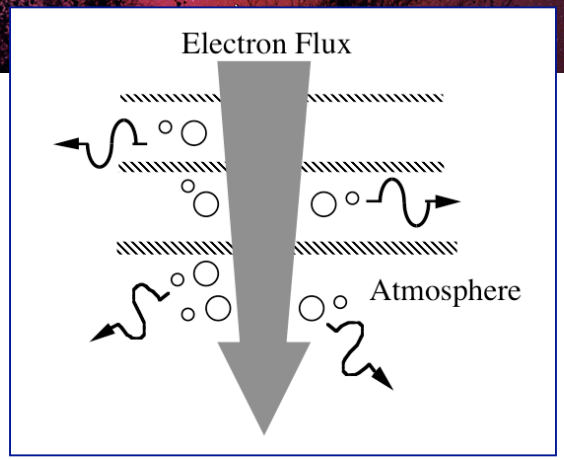

The aurora modifies the composition of the ionosphere.

Courtesy to Richard Collins of UAF

The Spectroscopy of Molecules vs. Atoms

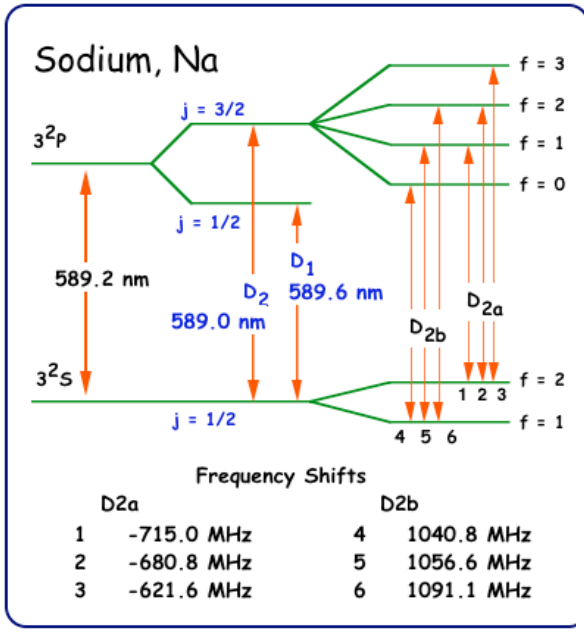

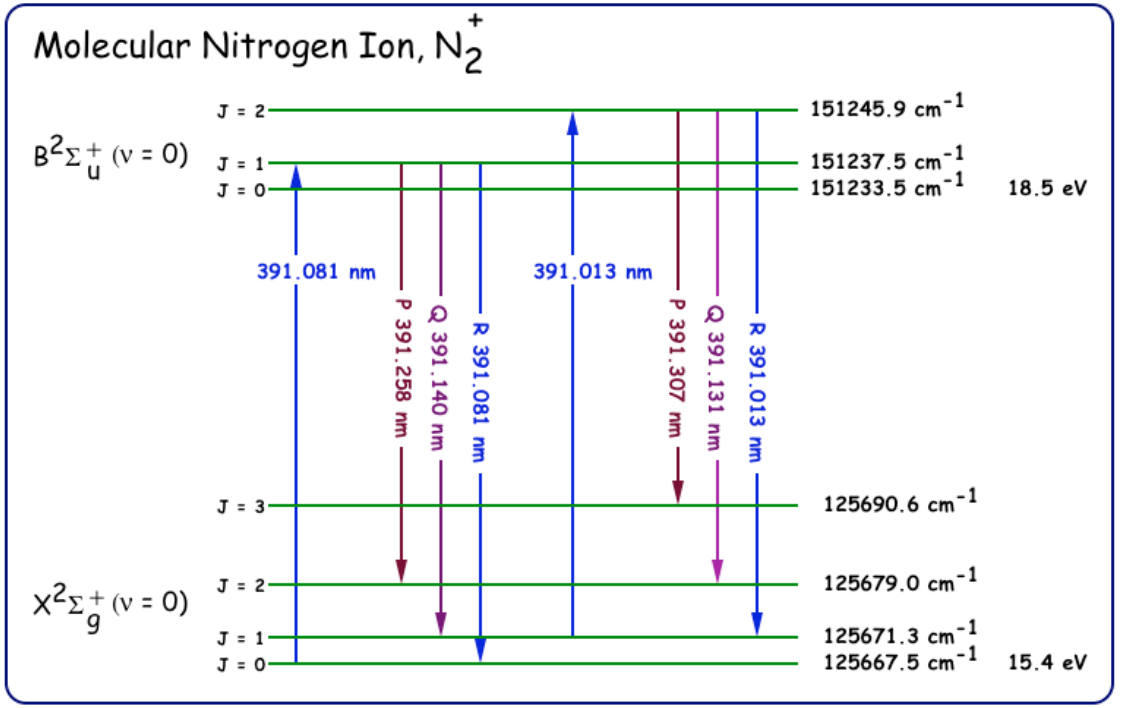

Molecular spectroscopy has vibrational and rotational states.

Courtesy to Richard Collins of UAF

N_2^+ Boltzmann Temperature Lidar

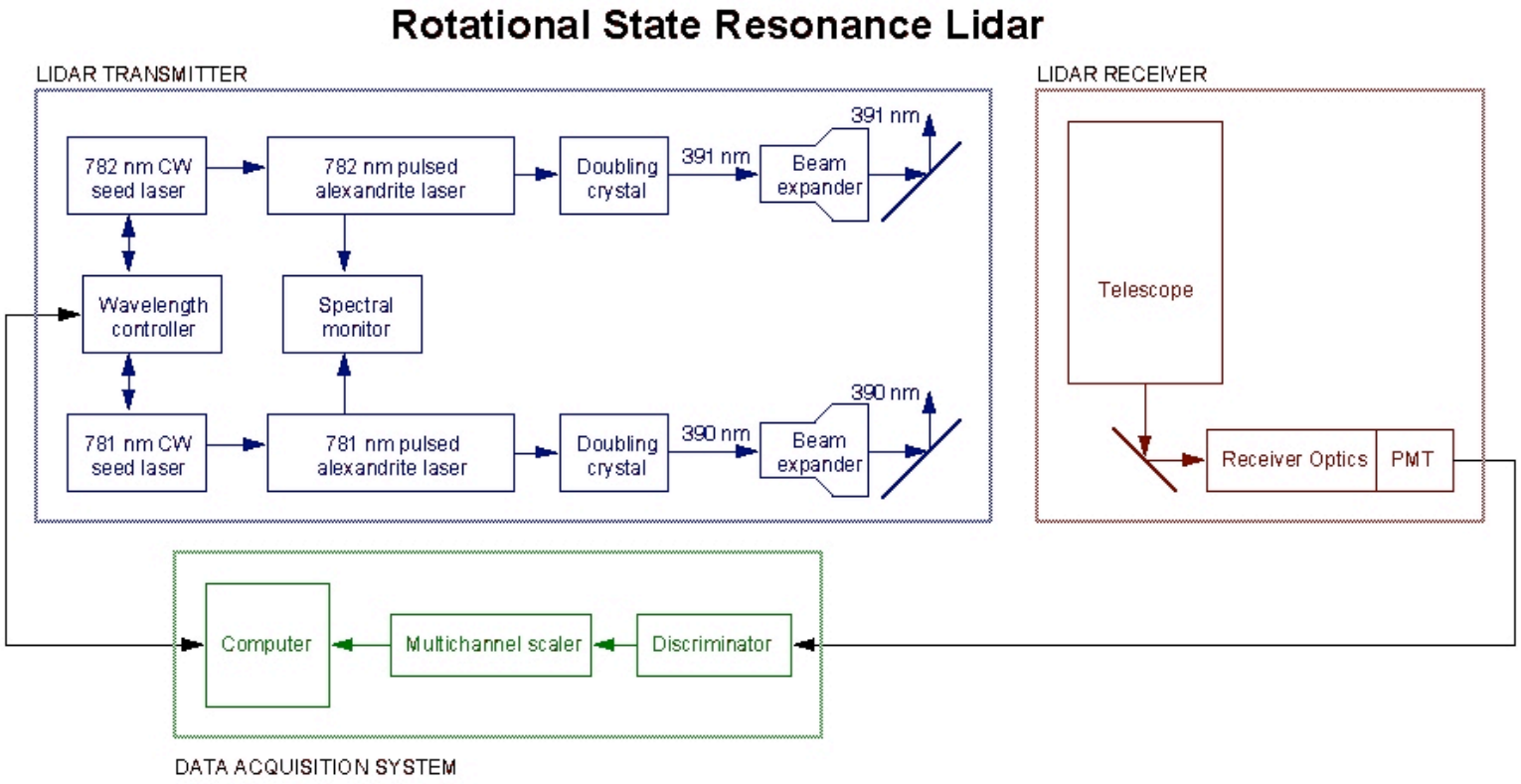

A dual laser lidar system employing solid-state lasers could be used to profile two rotational states simultaneously and hence study the energy deposition in the auroral ionosphere.

Courtesy to Richard Collins of UAF

Raman Scattering of N_2 and O_2

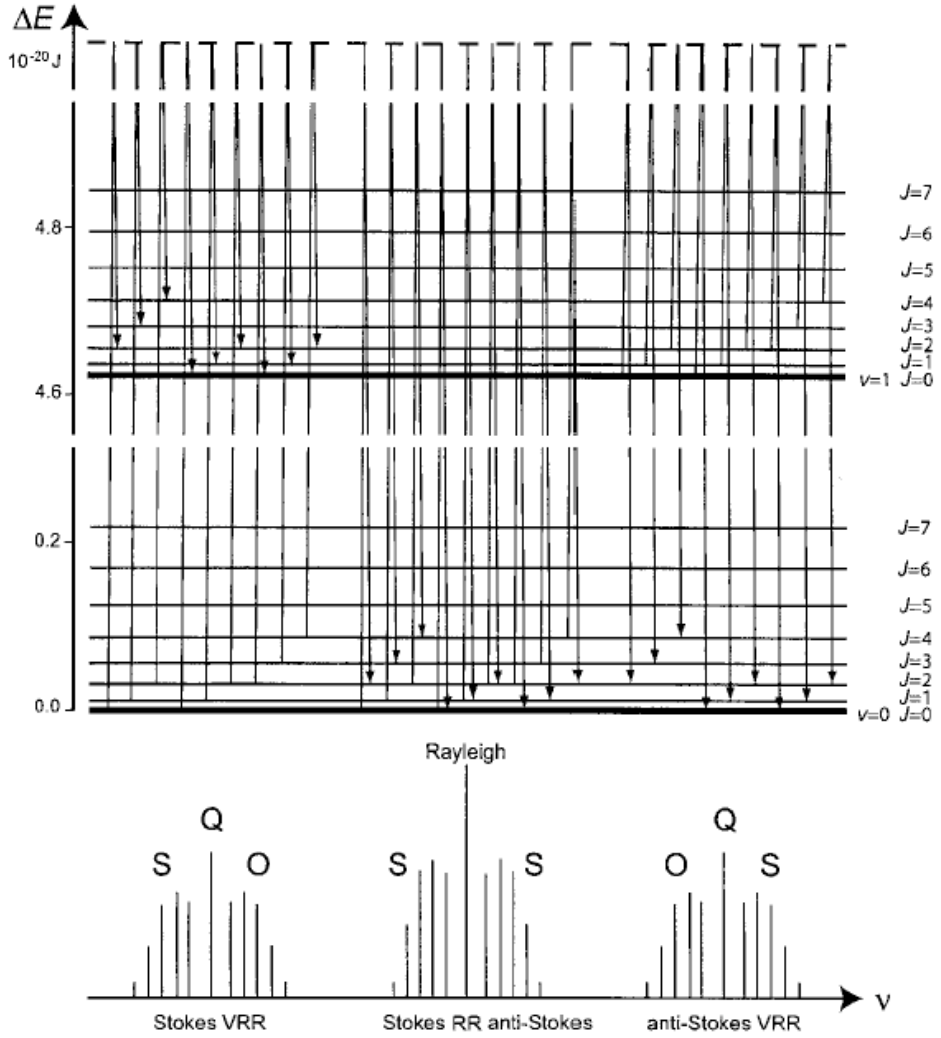

Fig. 9.1. Vibration–rotation energy levels of the N_2 molecule, Raman transitions, and resulting spectrum.

- Raman shift amount is independent of incident laser wavelength

Raman Scattering

- Volume backscatter coefficient for single Raman lines

$$\left(\frac{d\sigma}{d\Omega}\right)_J^{RR.VRR} = k_{\tilde{\nu}}(\tilde{\nu}_l \mp |\Delta\tilde{\nu}|)^4 \frac{g_N \Phi_J}{Q} \exp\left[-\frac{B_i h c_0 J(J+1)}{k_B T}\right]$$

Which is the product of the transition probability and the population on the initial energy state. So the temperature dependence comes from the population distribution - Boltzmann distribution law!

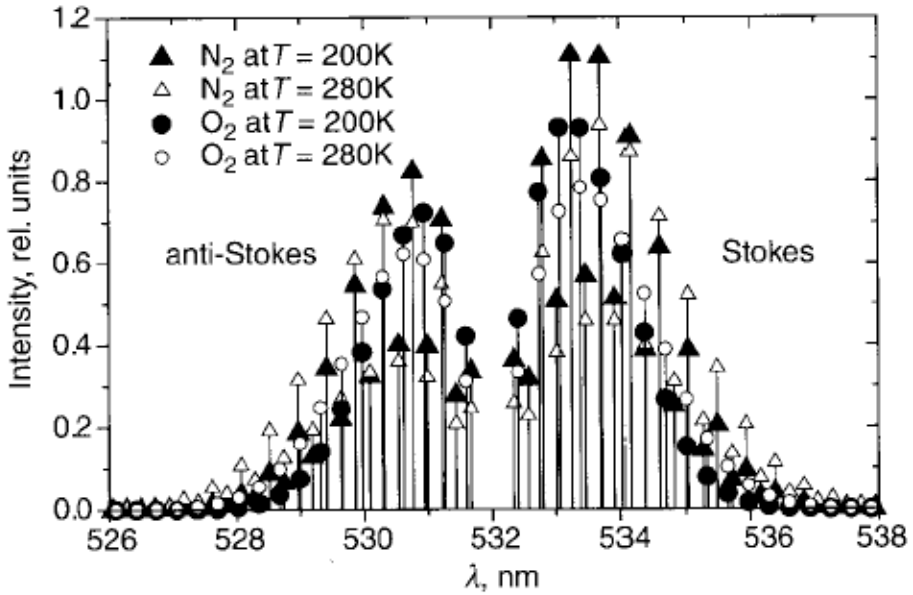

Rotation Raman Lidar

- Depending on what the initial energy state is, the line intensity can increase or decrease when temperature increases.
- If the initial energy state is one of the upper levels of the ground state, increasing in temperature will increase the population on the initial state, so the Raman line intensity will increase.
- If the initial energy state is the lowest level of the ground state, increasing temperature will decrease the population on the initial state, so the Raman line intensity will decrease.
- By measuring the intensity of two Raman lines with opposite temperature dependence, the ratio of these two lines is a sensitive function of atmospheric temperature.

$$Q(T, z) = \frac{S_{\mathrm{RR2}}(T, z)}{S_{\mathrm{RR1}}(T, z)}$$

Rotation Raman Lidar

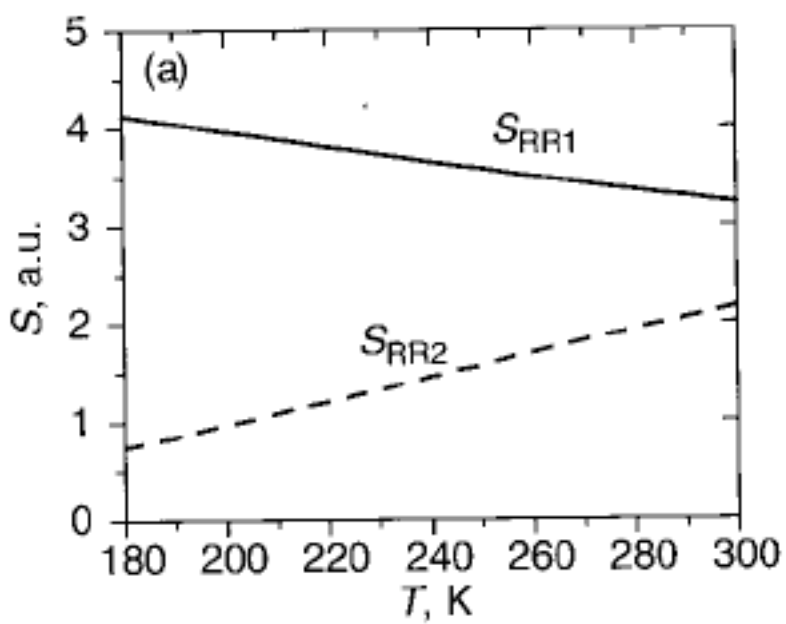

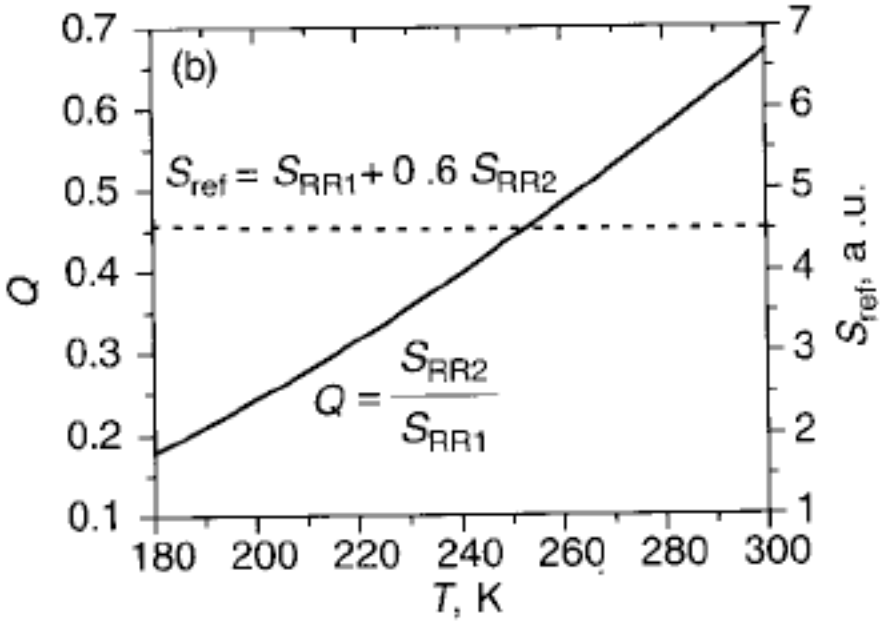

$$Q(T) = \frac{\sum_{i=O_2,N_2} \sum_{J_i} \tau_{RR2}(J_i)\eta_i \left(\frac{d\sigma}{d\Omega}\right)_{\pi}^{RR,i}(J_i)}{\sum_{i=O_2,N_2} \sum_{J_i} \tau_{RR1}(J_i)\eta_i \left(\frac{d\sigma}{d\Omega}\right)_{\pi}^{RR,i}(J_i)}$$

- Therefore, temperature can be derived from the ratio of two pure Rotational Raman line intensity. This is essentially the same principle as Boltzmann temperature technique!

Combined Rotation Raman and Elastic Scattering Lidar

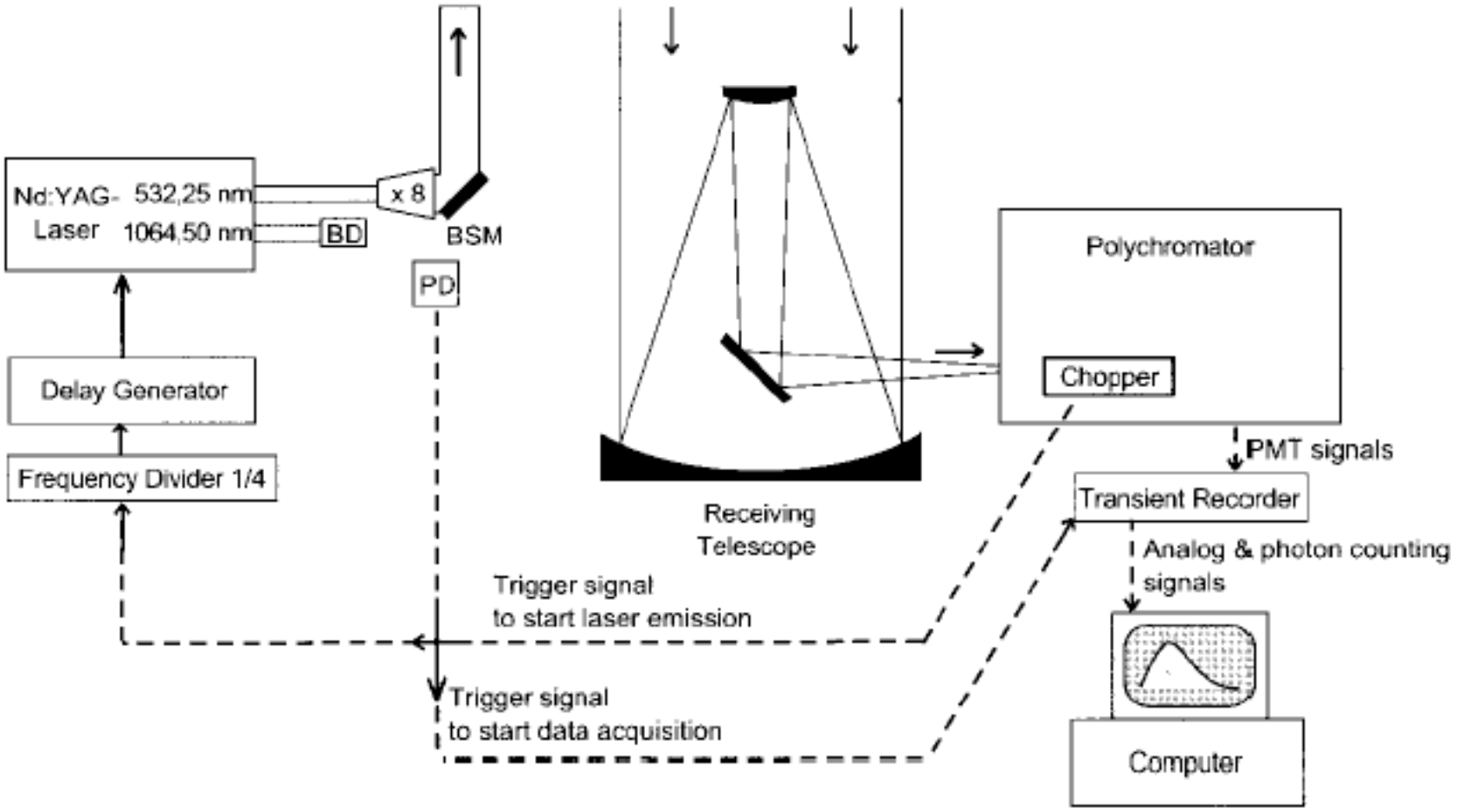

Rotation Raman + Elastic Lidar

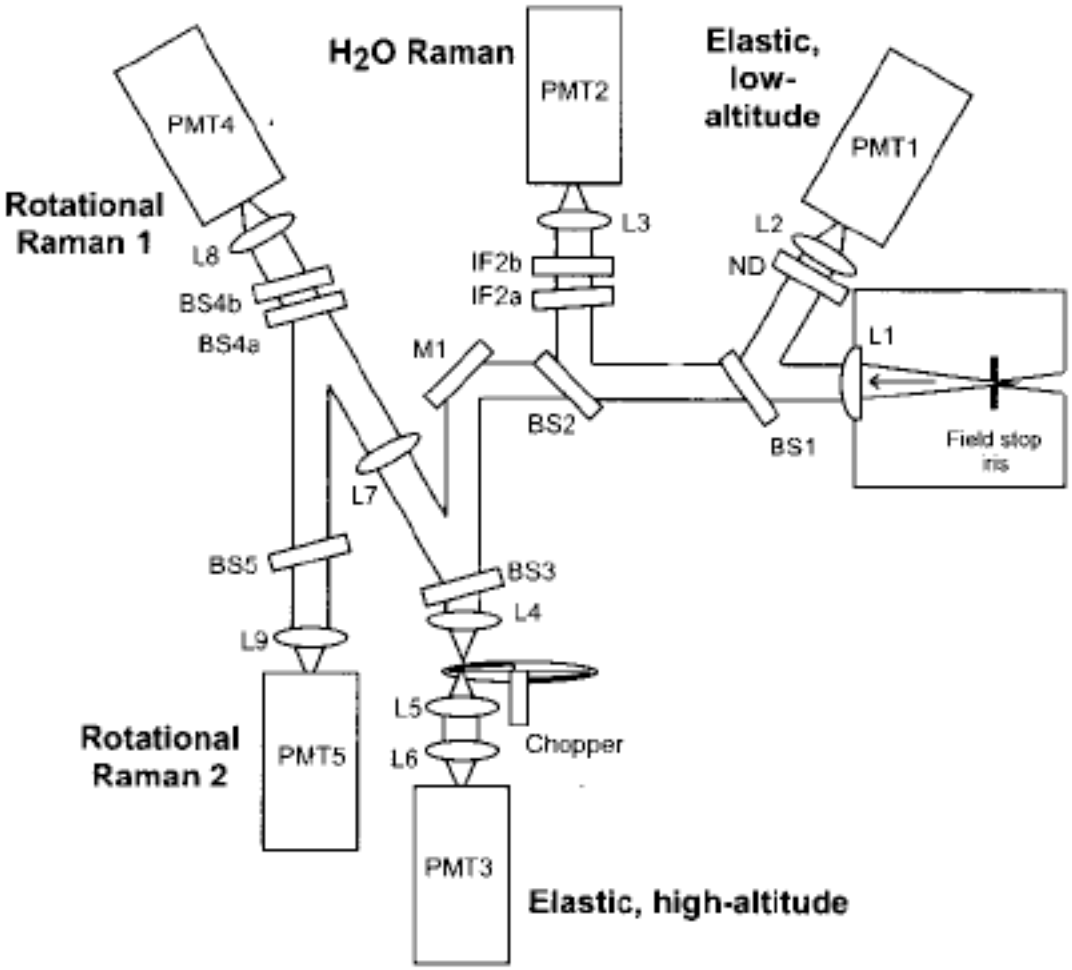

Lidar Polychromator

Results from Combined RR and Elastic Scattering Lidar

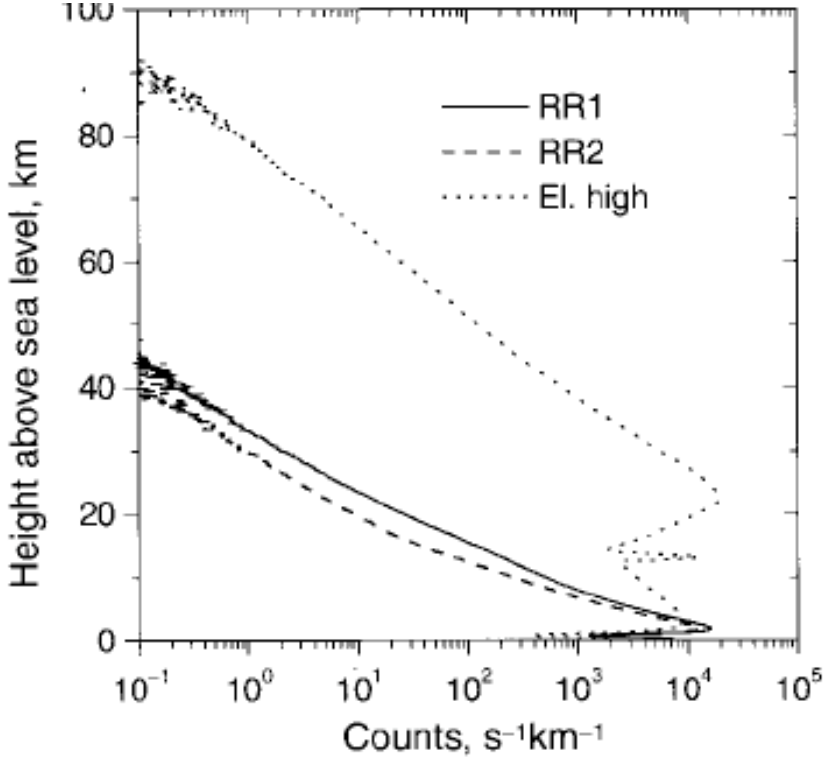

Fig. 10.11. Intensities of the RASC lidar signals for the temperature measurements: rotational Raman signals (RR1 and RR2) and high-altitude elastic signal (El. high). For this plot, 72 minutes (216,000 laser pulses) of nighttime lidar data were taken with a height resolution of 72 m, summed, the background was subtracted, and the data were finally smoothed with a sliding average of 360 m. The photon emission rate of the laser is $\sim 8 \times 10^{19}$ photons/s. In the high-altitude elastic signal, the effect of the chopper can be seen below ~25 km and the signature of a cirrus cloud in ~13 km height.

Results from Combined RR and Elastic Scattering Lidar

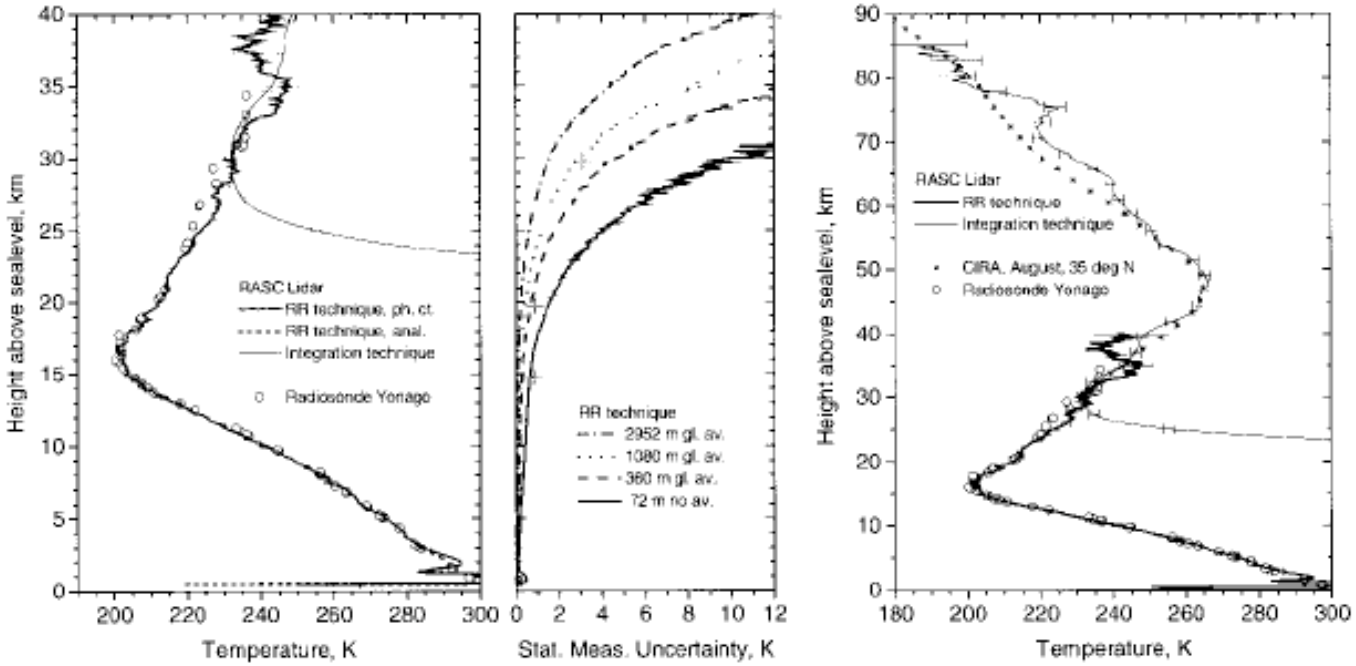

Fig. 10.12. Simultaneous temperature measurements with rotational Raman technique and with integration technique (signals see Fig. 10.11). Profiles of a climatological model atmosphere (CIRA-86 for 35°N and the month of the lidar measurements) and of a radiosonde are shown for comparison. Rotational Raman temperature data: height resolution of 72 m up to 15 km height, 360 m between 15 and 20 km height, 1080 m between 20 and 30 km height, and 2952 m above 30 km. Height resolution of the integration technique data is 2952 m. Error bars show the $1-\sigma$ statistical uncertainty of the measurements [48].

DIAL Temperature Technique

- Molecular absorption coefficient is temperature dependent: both the line strength and the lineshape are function of temperature.
- So by measuring the molecular absorption coefficient, it is possible to derive temperature if the molecular number density is known. For this purpose, O_2 is chosen because of its constant mixing ratio up to high altitude and suitable absorption lines.
- In the choice of suitable absorption line, a trade-off must be made between the high temperature sensitivity of the absorption cross-section (high for high initial energy state) and the suitable magnitude of absorption coefficient.
- Absorption coefficient is also dependent on pressure, making the temperature derivation more difficult.

Summary

- Boltzmann technique utilizes Maxwell-Boltzmann distribution of atomic or molecular populations along different energy levels, which is directly temperature dependent.
- The temperature-dependent population ratio is inferred through the intensity ratio of two resonance fluorescence lines whose lower energy levels are the two energy levels that we concern.
- The key is to find the right energy level diagrams that are suitable to this measurement - energy separation is not too large or too small, and wavelengths fall in the laser reachable range.
- Boltzmann technique can be applied to not only the Fe Boltzmann lidar but also potentially to other molecular species like N_2^+.
- Boltzmann technique is also used in rotational Raman lidar and in airglow temperature mappers, like Bomem.